Aquat Geochem
DOI 10.1007/s10498-016-9305-3

ORIGINAL PAPER

Benthic Oxygen Fluxes Measured by Eddy Covariance in Permeable Gulf of Mexico Shallow-Water Sands

Lindsay Chipman[1] · Peter Berg[2] · Markus Huettel[3]

Received: 5 April 2016 / Accepted: 8 October 2016

Abstract Oxygen fluxes across the sediment–water interface reflect primary production and organic matter degradation in coastal sediments and thus provide data that can be used for assessing ecosystem function, carbon cycling and the response to coastal eutrophication. In this study, the aquatic eddy covariance technique was used to measure seafloor–water column oxygen fluxes at shallow coastal sites with highly permeable sandy sediment in the northeastern Gulf of Mexico for which oxygen flux data currently are lacking. Oxygen fluxes at wave-exposed Gulf sites were compared to those at protected Bay sites over a period of 4 years and covering the four seasons. A total of 17 daytime and 14 nighttime deployments, producing 408 flux measurements (14.5 min each), were conducted. Average annual oxygen release and uptake (mean ± standard error) were 191 ± 66 and -191 ± 45 mmol m^{-2} day^{-1} for the Gulf sites and 130 ± 57 and -152 ± 64 mmol m^{-2} day^{-1} for the Bay sites. Seasonal variation in oxygen flux was observed, with high rates typically occurring during spring and lower rates during summer. The ratio of average oxygen release to uptake at both sites was close to 1 (Bay: 0.9, Gulf: 1.0). Close responses of the flux to changes in light, temperature, bottom current velocity, and wave action (significant wave height) documented tight physical–biological, benthic–pelagic coupling. The increase of the sedimentary oxygen uptake with increasing temperature corresponded to a Q_{10} temperature coefficient of 1.4 ± 0.3. An increase in flow velocity resulted in increased oxygen uptake (by a factor of 1–6 for a doubling in flow), which is explained by the enhanced transport of organic matter and electron acceptors into

Electronic supplementary material The online version of this article (doi:10.1007/s10498-016-9305-3) contains supplementary material, which is available to authorized users.

✉ Markus Huettel
mhuettel@fsu.edu

[1] Cooperative Institute for Research in Environmental Sciences, University of Colorado Boulder, Boulder, CO 80309, USA

[2] Department of Environmental Sciences, University of Virginia, Charlottesville, VA 22904, USA

[3] Department of Earth, Ocean and Atmospheric Science, Florida State University, Tallahassee, FL 32306, USA

Published online: 21 October 2016

the permeable sediment. Benthic photosynthetic production and oxygen release from the sediment was modulated by light intensity at the temporal scale (minutes) of the flux measurements. The fluxes measured in this study contribute to baseline data in a region with rapid coastal development and can be used in large-scale assessments and estimates of carbon transformations.

Keywords Eddy correlation · Eddy covariance · Oxygen flux · Gulf of Mexico · Permeable sediment · Inner shelf · Coastal zone

1 Introduction

Benthic oxygen flux is a key environmental parameter in marine systems, as it provides information on metabolic and oxidation processes and can be closely linked to the biogeochemical cycling of organic matter (Canfield et al. 1993; Glud 2008). Ultimately, most of the oxygen uptake in the sediment results directly from biological organic carbon decomposition; thus, oxygen flux depends on the availability and degradability of sedimentary organic matter. Within the sediment, aerobic carbon degradation by microbial communities and geochemical oxidation processes consume oxygen, and the rates of these processes together with the transport rates of electron acceptors and electron donors affect benthic oxygen fluxes. Where light reaches the sea floor, photosynthetic oxygen production by benthic algae, photoautotrophic bacteria, coral reefs, and aquatic plants (e.g., seagrass) also contributes to the overall oxygen flux (Cahoon 1999; Gattuso et al. 2006).

Sediment oxygen dynamics can be highly variable, especially in heterogeneous shallow coastal regions, where multiple factors such as bottom water oxygen concentration, carbon availability, temperature, light, hydrodynamics, sediment composition, sedimentation rates, and benthic fauna influence oxygen dynamics (Glud 2008; Jahnke et al. 2005). The extent to which each factor contributes to the benthic oxygen flux is affected by site characteristics and time of measurement. In shallow coastal sites, microphytobenthos oxygen production at an apparently bare sediment surface layer can exceed benthic oxygen uptake and lead to positive oxygen fluxes, i.e., upward directed fluxes into the water column (Berg et al. 2013; Jahnke et al. 2008). The abundance and activity patterns of benthic fauna (e.g., demersal fish, crustaceans, and polychaetes) influence the magnitude and temporal changes of oxygen flux through their activity patterns and metabolism (Forster et al. 1999; Mermillod-Blondin et al. 2005; Wenzhofer and Glud 2004). In coastal regions with permeable sediments, bottom currents can strongly enhance oxygen transport into the seabed (Huettel and Gust 1992; Huettel and Webster 2000; Jahnke et al. 2000; Ziebis et al. 1996b). Likewise, surface gravity waves can increase transport of oxygen into shallow-water permeable sediments through the process known as the subtidal pump (Riedl et al. 1972), where oscillatory pressure gradients resulting from the passage of waves cause pore-water exchange. Such pore-water transport affects the distribution and interactions of biologically and geochemically reactive solutes and particles, and thereby the benthic oxygen consumption. Although the carbon content of coastal sands is typically low, they can have high turnover rates of reactive carbon facilitated by high permeability and pore-water exchange, resulting in substantial oxygen fluxes (Berg et al. 2013; Chipman et al. 2010; Huettel and Rusch 2000; Jahnke et al. 1996; Ziebis et al. 1996a).

Because currents, wave action, light, and fauna can have profound effects on sedimentary oxygen dynamics, it is critical to minimize disturbances of in situ conditions when measuring benthic fluxes. This can be accomplished with the aquatic eddy covariance method, which allows determining benthic fluxes non-invasively through simultaneous measurements of vertical velocity changes due to turbulence and associated variations in the oxygen concentration above the sediment surface, and subsequently correlating them (Berg et al. 2003). Compared to traditional methods for measuring benthic oxygen fluxes, such as chamber incubations and microprofiling across the sediment–water interface, the eddy covariance technique causes little or no disturbance of the natural light and flow conditions or benthic organisms, and thereby allows the examination of these parameters on oxygen flux under realistic in situ conditions.

Only few measurements of oxygen flux dynamics under non-disturbed in situ conditions exist for permeable sediments. In this paper, we report measurements of benthic oxygen release and uptake in shallow-water permeable coastal sands in the northeastern Gulf of Mexico. We investigated seasonal flux changes and how light, flow, wave height, and temperature, influence oxygen flux. We determined the range and variability of the fluxes over a 4-year period and compared the values with those from similar environments previously reported in the literature. Our main research questions are:

1. What are the typical magnitude, range, and variability of oxygen fluxes in coastal permeable sediments of the northeastern Gulf of Mexico on time scales ranging from hours to seasons, and how do these fluxes compare to those at other sites?
2. What are the major factors influencing oxygen flux at these sites, and how do changes in these factors affect the magnitude of oxygen fluxes?

The flux data produced in this project contribute to baseline data for a coastal environment for which no oxygen flux data exist and that presently is facing rapid development.

2 Methods

2.1 Study Sites

Our study included five sites in the northeastern Gulf of Mexico on the Florida coast: St. George Island Gulf (1 and 2), St. George Island Bay, St. Joseph Bay, and Pensacola Beach (Fig. 1A). Three of the sites (St. George Gulf 1 and 2 and Pensacola Beach) were exposed to the open ocean, whereas the other two sites (St. George Bay and St. Joseph Bay) were located in bays protected from the open ocean. The exposed sites experienced more dynamic forcing from ocean waves and currents than the bay sites; however, current and wave conditions at all sites were relatively calm (wind speed <4 m s^{-1}, currents <30 cm s^{-1}, significant wave height <50 cm), which is typical for the northeastern Gulf of Mexico (Zavala-Hidalgo et al. 2014). The mean tidal range in the northeastern Gulf area is ~ 60 cm, and the tidal currents at all sites except St. George Gulf site 2 are weak (<10 cm s^{-1}) (He and Weisberg 2002). The study region is influenced by discharge from the Apalachicola River, which follows a seasonal cycle with maximum discharge rates in spring and minimum rates in summer (Fig. 1B). The nutrient input by the river affects primary production in the Bay and adjacent coastal environments (Morey et al. 2009; Santema et al. 2015). The surface sediments at all the sites consist of well-sorted quartz

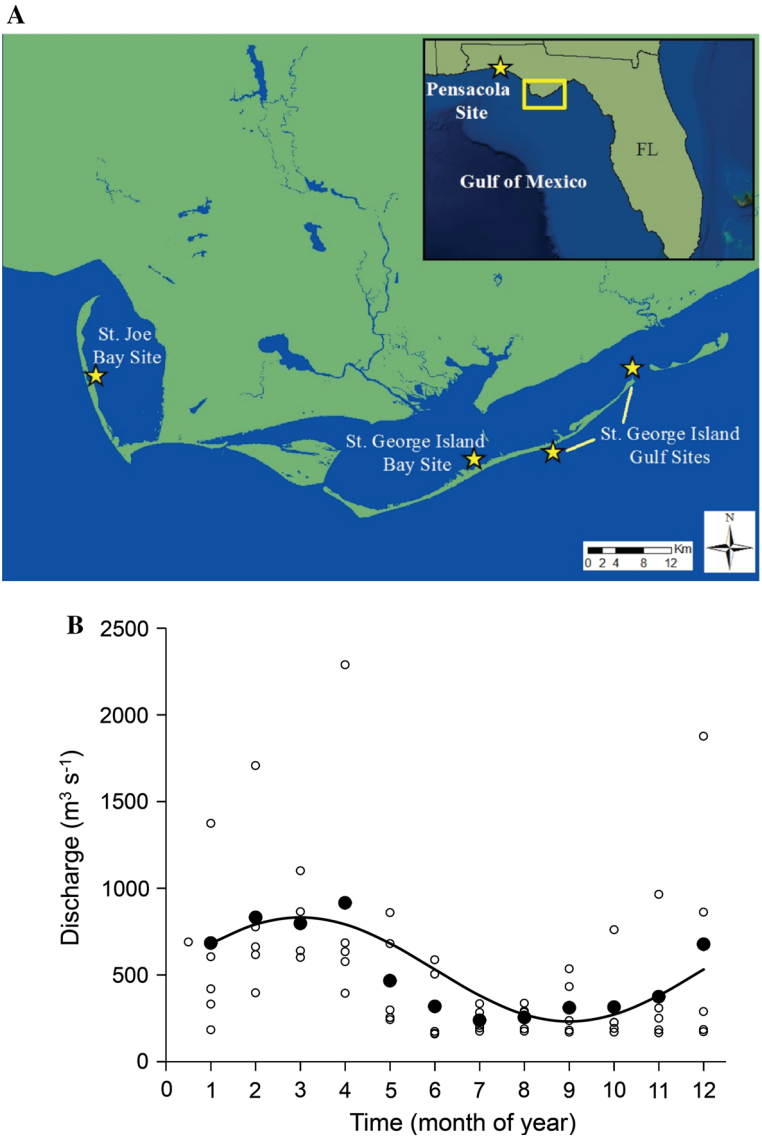

Fig. 1 **A** Study sites in the Northeastern Gulf of Mexico marked by *yellow stars*: Pensacola Beach, St. Joe Bay, and St. George Island Gulf and Bay sites. **B** Apalachicola River discharge during the study period (2007–2011) with an average maximum in March (800 m^3 s^{-1}) and average minimum in August (250 m^3 s^{-1}). *Solid circles* represent monthly averages during the study period. The trend *line* represents a sinusoidal fit to the data. Data from USGS (http://waterdata.usgs.gov/nwis/)

sands. The geographic coordinates of the sites and their characteristics are listed in Table 1.

Exposed sites: The St. George Island Gulf Site 1 was located on the ocean side of the barrier island, whereas the St. George Island Gulf Site 2 was near the inlet at the east end of the Bay and characterized by stronger tidal flows and coarser, more permeable sands

Table 1 Geographic coordinates, water depth, and characteristics of the sandy sediments at our study sites

Site (name)	Lat (N)	Long (W)	Mean water depth (m)	Median grain size (μm)	Permeability (m^2)	Organic content [% (dw/dw)]	$\delta^{13}C_{(PDB)}$ (‰)
Gulf sites (exposed)							
St. George Island Gulf 1	29°41′10″	−84°47′20″	2	223 ± 44	$2.4 \times 10^{-11} \pm 1.0 \times 10^{-11}$	0.10 ± 0.02	−22.12 ± 0.62
St. George Island Gulf 2	29°46′23″	−84°41′45″	2	325 ± 78	$5.6 \times 10^{-11} \pm 1.0 \times 10^{-11}$	0.05 ± 0.02	n/a
Pensacola Beach	30°19′30″	−87°10′31″	2	448 ± 56	$6.7 \times 10^{-11} \pm 1.6 \times 10^{-13}$	0.02 ± 0.01	n/a
Bay sites (protected)							
St. George Island Bay	29°39′5″	−84°52′08″	2	211 ± 16	$1.3 \times 10^{-11} \pm 0.5 \times 10^{-11}$	0.19 ± 0.11	−18.65 ± 2.03
St. Joseph Bay	29°45′56″	−85°24′11″	1.5	286 ± 56	$4.43 \times 10^{-11} \pm 4.13 \times 10^{-13}$	0.05 ± 0.02	n/a

Error estimates represent one standard deviation. $\delta^{13}C$ is a measure of the ratio of stable isotopes ^{13}C:^{12}C, and Pee Dee Belemnite (PDB) is the reference material

compared to Gulf site 1 (Table 1). Because the average flow and wave height at this site were comparable or higher than those at the other Gulf sites, we classified this site as an open-ocean site.

The Pensacola Beach site was located on the Gulf of Mexico side of Santa Rosa Island and exposed to the open ocean. In April 2010, the BP Deepwater Horizon oil spill reached the beaches in this area, contaminating the water and sediment with oil. The beach had been cleaned by the time we performed our deployment here, and concentrations of petroleum hydrocarbons in water and sediment were not significantly different from pre-spill conditions (Snyder et al. 2014a, b).

Protected sites: The St. George Island Bay Site was situated on the side of St. George Island facing Apalachicola Bay and thus is protected from the open Gulf of Mexico. The bay has an average water depth of 3 m, and water currents are dominated by the tides and wind-driven currents (Huang and Spaulding 2002).

The St. Joseph Bay site was situated on the protected east side of St. Joseph Peninsula, in St. Joseph Bay. This bay is bounded by the mainland to the east, Cape San Blas to the south, and the St. Joe Peninsula to the west, and thus the water in the bay is relatively calm. Similar to the St. George Island bay site, the water currents at the St. Joseph Peninsula site are dominated by the tides and wind-driven currents.

2.2 Eddy Covariance System

Our eddy covariance system was designed after the instrument described by Berg and Huettel (2008) and consisted of a Nortek Vector acoustic doppler velocimeter (ADV) and a fast-response oxygen microelectrode connected to a custom-built picoampere meter

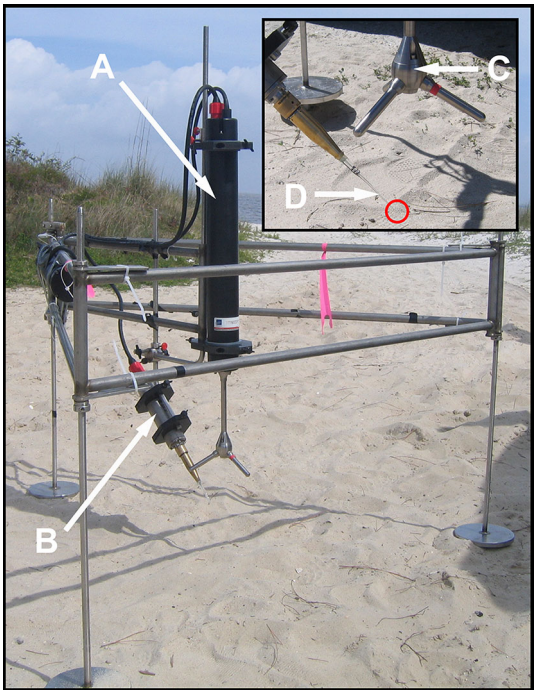

Fig. 2 Components of our eddy covariance system including the ADV (*A*) and picoampere meter with attached microelectrode (*B*). The *inset* shows a close up of the ADV sensor head with its three measuring prongs (*C*) and the Clark-type microelectrode (*D*). The *red circle* indicates the approximate position of the tip of the microelectrode next to the measuring volume of the ADV. All instruments are mounted on a lightweight stainless steel tripod

(Fig. 2). The ADV recorded the three water velocity components (x, y, z) and oxygen data simultaneously at a rate of 64 Hz. The Clark-type microelectrode equipped with a guard cathode was optimized with a small tip (<20 μm) and an optimal distance between the tip and measuring cathode to achieve low stirring sensitivity and fast response time (Gundersen et al. 1998). The accuracy of the absolute oxygen concentration measurements was ±0.2 % of air saturation, or approximately ±0.5 μmol L^{-1} based on microelectrode readings of standards verified by multiple Winkler titration (Grasshoff et al. 1999). The effective precision in our measurements was at least one order of magnitude larger because the calculation of eddy fluxes relies on relative concentration changes. The ADV, picoampere meter, and electrode were mounted on a lightweight frame and positioned so that the tip of the electrode was next to the measuring volume of the ADV (14 mm height, 14 mm diameter). The measuring height was set at approximately 10 cm above the seafloor for all deployments. Measurements were made at 14.5 min intervals, separated by a 30-s pause that allowed the sensor electronics to optimize the output range. Drift-stable Hach oxygen optode sensors and/or an Aanderaa Seaguard with optical oxygen sensor were used in all deployments to measure ambient oxygen concentrations every 5 min. These ambient oxygen measurements provided reference values for the microelectrode calibration. The Seaguard also recorded significant wave height. Salinity was measured during each deployment with a YSI handheld meter. A Licor PAR light sensor and/or Hobo sensors, attached to the frame recorded light intensity [in μE m^{-2} s^{-1} (Licor), lum m^{-2} (Hobo)] and temperature (°C) at 5-min intervals (Table 2).

2.3 Data Processing

The 64 Hz raw data were grouped into 16 Hz data to reduce signal noise, and oxygen fluxes were extracted from each 14.5 min measuring interval using the EddyFlux software (P. Berg, unpublished). Flux was calculated as $F = \overline{u_z' C'}$, where u_z' is the fluctuating component of vertical velocity away from the mean, and C' is the fluctuating component of concentration away from the mean (Berg et al. 2003, 2009). Means for each 14.5-min interval were calculated using the running averaging (Lee et al. 2004; Berg et al. 2009). A 60-s window was used to calculate the running average used in flux calculations. This window size was chosen to include flux-contributing eddies (e.g., Fig. 6), while excluding factors such as drift and changes in mean velocity and oxygen concentration. A 14.5-min window was used as the flux-averaging time because the window should be ~5 to 10 times that of the largest eddy time scale to include multiple replicates of the lowest frequencies (Businger 1986; Lorrai et al. 2010; Lorke et al. 2013).

When extracting EC fluxes, rotation of the velocity field is recommended to correct for instrument tilt relative to the seafloor (Lorke et al. 2013), but in environments with surface waves or low/unsteady flow, rotation can result in faulty fluxes and should be used with caution (Reimers et al. 2012; Rheuban et al. 2014a). We calculated and compared rotated with non-rotated fluxes using a two-sample Kolmogorov–Smirnov test. In the case of no significant difference between the two sets of flux values, non-rotated data were used for all subsequent calculations (Rheuban et al. 2014a; Long et al. 2015). For cases in which rotation resulted in significantly different fluxes ($p < 0.05$), the data were further examined. If the rotated flux values were orders of magnitude higher and/or exhibited high variation compared with non-rotated values, the rotation was deemed unsuitable and non-rotated data were used in subsequent calculations; otherwise, rotated data were used accordingly.

Table 2 Averages and ranges of environmental parameters during each deployment. *v* mean current velocity , O_2 water oxygen concentration, *PAR* photosynthetically active radiation, *T* water temperature, *SWH* significant wave height

Site	Date	*v* (cm s^{-1})	O_2 (μmol L^{-1})	PAR (μmol photons m^{-2} s^{-1})	*T* (°C)	SWH (m)
PB	July 10	2.7 ± 1.2 0.8–5.5	214 ± 22 187–257	15 ± 37 0–165	29.4 ± 5 23.7–37.7	0.22 ± 0.02 0.19–0.27
PB	Oct 10	1.8 ± 0.5 1.3–2.5	257 ± 4 252–264	1 ± 2 0–6	25.3 ± 0.1 25.2–25.5	0.41 ± 0.02 0.38–0.43
PB	Sept 11	1.5 ± 0.9 0.7–3.2	232 ± 3 227–237	370 ± 128 155–493	28.9 ± 0 28.9–28.9	0.27 ± 0.03 0.24–0.31
PB	Dec 11	2.6 ± 0.1 2.5–2.7	278 ± 2 275–281	571 ± 131 362–682	15.2 ± 0 15.1–15.2	0.2 ± 0.01 0.18–0.21
PB	Dec 11	2.0 ± 0.5 1.1–2.7	276 ± 1 274–278	0 ± 0 0–0	16 ± 0.2 15.7–16.3	0.25 ± 0.02 0.22–0.28
SGB	Mar 07	1.6 ± 0.5 1.1–2	305 ± 9 297–313	N/A	23.6 ± 0.1 23.5–23.7	N/A
SGB	Mar 07	2.3 ± 0.3 1.9–2.8	202 ± 5 194–210	4 ± 1 3–5	23.4 ± 0.1 23.1–23.6	N/A
SGB	Mar 07	2.3 ± 0.8 0.8–3.5	225 ± 15 204–248	11 ± 5 0–17	24.2 ± 1 2 1.6–26.2	N/A
SGB	Apr 08	3.0 ± 1.8 0.8–5.6	276 ± 31 229–305	22 ± 14 8–47	N/A	N/A
SGB	Apr 08	2.3 ± 1 0.9–4.3	259 ± 27 201–302	24 ± 14 3–47	N/A	N/A
SGB	Apr 08	2.6 ± 0.9 0.6–4.7	183 ± 29 152–262	0 ± 0 0–0	N/A	N/A
SGB	Mar 09	4.4 ± 0.6 3.3–5	223 ± 15 207–240	88 ± 53 24–178	14.1 ± 0.2 13.8–14.5	N/A
SGB	Mar 09	2.5 ± 0.9 1.5–5	171 ± 16 150–201	1 ± 3 0–18	12.7 ± 0.7 11.4–13.7	N/A
SGB	Apr 09	6.8 ± 0. 9 6–8.2	226 ± 10 210–236	836 ± 461 56–1196	N/A	N/A
SGB	Apr 09	5.5 ± 0.4 4.8–5.8	194 ± 1 193–195	1 ± 0 1–1	N/A	N/A
SGB	May 10	2.3 ± 0.6 1.5–2.8	219 ± 19 205–250	50 ± 5 45–56	24.8 ± 0.1 24.7–25	0.01 ± 0 0.01–0.02
SGB	May 10	1.9 ± 0.7 0.4–3.4	240 ± 23 213–286	0 ± 1 0–3	24.9 ± 0.1 24.6–25.1	0.02 ± 0.01 0–0.03
SGB	June 11	1.1 ± 0.6 0.2–2.1	212 ± 10 199–225	0 ± 0 0–0	30.5 ± 0.1 30.4–30.7	0.07 ± 0.06 0.03–0.2
SGB	June 11	0.3 ± 0.1 0.1–0.4	171 ± 5 165–175	30 ± 19 9–56	29.9 ± 0.1 29.8–30	0.15 ± 0.01 0.14–0.17
SGB	June 11	0.6 ± 0.4 0.2–2	185 ± 6 172–195	0 ± 0 0–0	30.1 ± 0.3 29.8–30.8	0.08 ± 0.04 0.02–0.16
SGEB	June 11	4.8 ± 0.3 4.6–5.1	213 ± 0 213–213	3 ± 3 1.85–6.3	30.3 ± 0.1 30.2–30.3	0.38 ± 0.01 0.37–0.38
SGEB	June 11	12.1 ± 3 7.2–16	241 ± 6 236–254	81 ± 54 7–168	30.9 ± 0.2 30.6–31.3	0.18 ± 0.06 0.1–0.26
SGEB	July 11	9.7 ± 7.8 3.8–25.1	232 ± 11 210–239	0 ± 1 0–1	29.7 ± 0 29.7–29.8	0.04 ± 0.01 0.03–0.06

Table 2 continued

Site	Date	v (cm s^{-1})	O_2 (μmol L^{-1})	PAR (μmol photons m^{-2} s^{-1})	T (°C)	SWH (m)
SGG	Mar 07	8.1 ± 0.8 7.0–9.3	237 ± 6 228–242	N/A	22.9 ± 0.1 22.8–23.1	N/A
SGG	Mar 07	5.3 ± 0.8 3.9–6.3	227 ± 4 218–232	14 ± 2 10–18	23.6 ± 0.4 23.1–24.3	N/A
SGG	Mar 09	2.4 ± 0.5 1.7–2.9	326 ± 1 325–327	397 ± 718 17–1670	16.8 ± 2.9 14.9–21.7	N/A
SGG	Mar 09	6.2 ± 7.9 1.6–15.3	335 ± 2 333–337	0 ± 0 0–0	14.2 ± 0.2 14–14.3	N/A
SGG	Apr 09	10.8 ± 1 10.1–11.5	243 ± 0 242–243	1111 ± 45 1079–1143	N/A	N/A
SGG	Apr 09	11.3 ± 1.6 9.3–13.4	233 ± 3 232–238	1 ± 0 1–1	N/A	N/A
SGG	June 09	10.2 ± 1.9 8–13.3	254 ± 2 252–258	7 ± 3 3–11	29.7 ± 0.6 28.9–30.4	0.44 ± 0.01 0.42–0.44
SGG	June 09	4 ± 0.8 2–5.2	218 ± 10 205–237	0 ± 0 0–0	27.2 ± 0.4 26.8–27.7	N/A
SGG	June 10	2.7 ± 0.9 1.3–4.9	199 ± 10 180–211	NA	28.3 ± 0.5 27.6–29.1	N/A
SJB	Feb 11	0.8 ± 0.2 0.4–1.4	315 ± 19 287–352	0 ± 0 0–0	10.7 ± 1.1 8.7–12.3	0.2 ± 0.03 0.16–0.26

PB Pensacola Beach, *SGB* St. George Bay, *SGEB* St. George East Bay, *SGG* St. George Gulf, *SJB* St. Joseph Bay

Noise in electrode and ADV signals typically is random and cancels out in the flux calculation (Lorrai et al. 2010). Signal jumps or irregularities are often caused by particles hitting the sensor and were identified by visually inspecting the data for jumps noticeably higher in magnitude than random noise and that occur simultaneously with nonlinear cumulative fluxes. When a signal anomaly is extreme enough to influence the resulting flux calculation, it is manifested as a nonlinearity or jump in the cumulative flux. Thus, the cumulative fluxes were examined for nonlinearity, and where a large anomaly was present, the corresponding O_2 and/or velocity signal was corrected by replacing signal or few-point jumps with the average of ±10 surrounding data points; for clustered numerous jumps or long disruptions, the interval was discarded. Discarded data were not included in the average values, though corrected signals were used in the flux calculations and included in the means. This process for checking data quality has been used in several other eddy covariance studies (e.g., Hume et al. 2011; Berg et al. 2013; Long et al. 2013).

The sizes and frequencies of the eddies carrying the flux signal varied with the environment and instrument setup (e.g., sediment roughness, current velocity, water depth, measuring height). To determine the ranges of the flux-carrying eddy frequencies, cumulative co-spectra of the oxygen concentration and vertical velocity were calculated (Berg et al. 2003; Lee et al. 2004) using the Spectra software (P. Berg, unpublished). These spectra reveal the frequencies contributing to the eddy flux, the suitability of the oxygen sensors' response time for measuring all the turbulent fluctuations, whether waves contributed to the flux, and whether the measuring window was long enough to capture lower frequencies (Chipman et al. 2012; Reimers et al. 2012). It is possible that a fraction of the eddy signal is lost when measurements are made under high flow, although high

frequencies (>1 Hz) generally do not contribute to a large portion of the flux (Donis et al. 2015). We examined this possibility by comparing the cumulative co-spectra for intervals during which mean velocity exceeded 15 cm s^{-1} and found that the spectrum of frequencies contributing to the flux remained in the same frequency range with relatively little effect of the current velocity on that range (Fig. S2).

The measured oxygen fluxes were classified as 'oxygen release' or 'oxygen uptake' based on the direction of the flux. Oxygen release (by photosynthesizing organisms at the sediment surface) is listed as positive fluxes measured during the day (corresponding to >1 % maximum normalized light for each deployment or after sunrise), and oxygen uptake (by sedimentary geochemical and biological oxidation processes) as negative fluxes measured at night (corresponding to <1 % maximum normalized light for each deployment or after sunset). The data were further grouped into 'Bay' sites (St. George Bay and St. Joseph's Bay) and 'Gulf' sites (St. George Gulf Sites 1 and 2, and Pensacola Beach) according to hydrodynamics and sediment type (Table 1). Grouped data were used to evaluate temporal patterns and balance of oxygen release to uptake, which could not be determined for individual sites due to discontinuity of data. We used the vernal equinox (March 20) as the starting day for spring and the summer solstice (June 20/21) as the starting day for summer. Fall measurements in 2011 began 11 days prior to the autumnal equinox (September 22/23), marking our starting day for fall to account for restrictions imposed by weather. The winter solstice (December 21/22) marked the beginning of the winter season. Field measurements were conducted between March 2007 and June 2011, and the deployments varied in length from 2 to 20 h.

3 Results

A total of 31 deployments were used in the analyses presented here, including a total of 408 fluxes, each based on a 14.5-min measuring interval. An example of a dataset produced by a successful eddy covariance deployment is shown in Fig. 3. The oxygen fluxes measured at our study sites varied between seasons and were modulated by light, bottom current velocity, wave action, and temperature. The mean and range of the calculated fluxes from all deployments are shown in Table 3. Plots of general environmental parameters including mean velocity, O_2, temperature, light, and wave height for the deployments are shown in Fig. S1.

The seasonally averaged oxygen release and uptake combined from all study sites are shown in Fig. 4. The flux magnitudes at the Gulf and Bay sites were not significantly different (based on a Student's *t* test) due to the high variability in the data. At the Bay sites, the average benthic oxygen release was highest during spring (207 ± 50 mmol m^{-2} day^{-1}) (mean ± standard error) and oxygen uptake was greatest during winter (−242 ± 207 mmol m^{-2} day^{-1}), corresponding to 12-fold and eightfold higher fluxes than during summer. Fall data are not available for the Bay site due to adverse weather conditions during the measuring campaigns. At the Gulf sites, oxygen uptake was highest during spring (−448 mmol m^{-2} day^{-1}), 11-fold higher than during winter, and release was highest in the fall (363 mmol m^{-2} day^{-1}), fivefold higher than during summer. The release to uptake ratios for days for which both values were available ranged from 0.1 to 2.7, with annual values of 0.9 for the Bay and 1.0 for the Gulf sites.

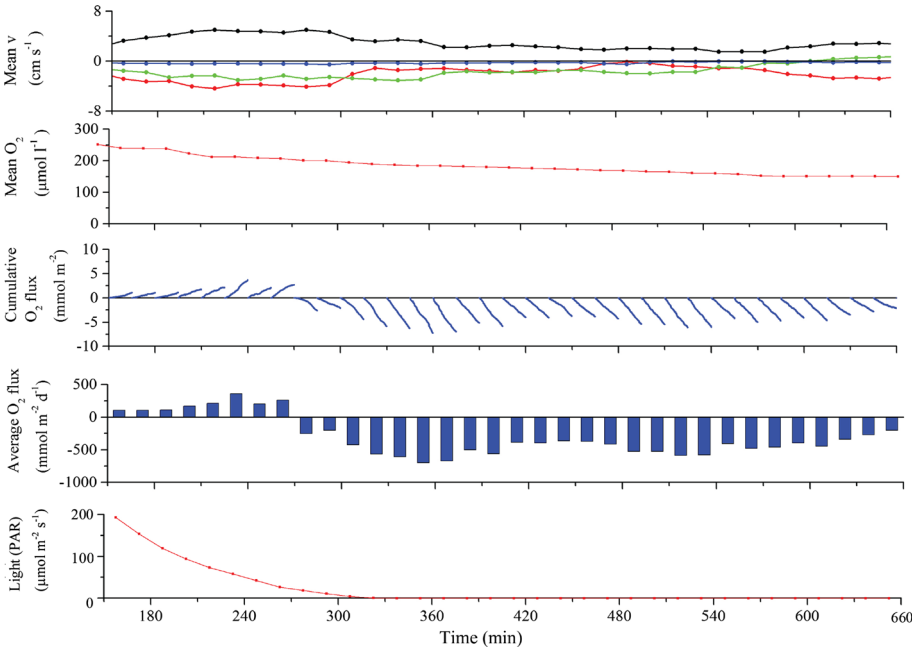

Fig. 3 Example of an eddy covariance dataset measured at the St. George Bay site in March 2009. The *uppermost panel* depicts the three flow velocity components (*green* and *red* are the horizontal components, *blue* the vertical component) and the average flow velocity (*black line*). The *second panel* depicts the oxygen concentration measured by the microelectrode. The *third panel* shows the accumulated instantaneous fluxes for each 14.5-min period, and the *fourth panel* depicts the mean oxygen flux for each 14.5-min interval. The *lowest panel* depicts light intensity at the seafloor. The observed reversal of the flux at 270 min coincided with sunset and was caused by the ending of photosynthetic oxygen production

3.1 Influence of Environmental Factors

Changes in environmental factors caused short-term variations in oxygen fluxes, resulting in relatively large variations in the flux values within deployments (e.g., 74 % coefficient of variation for release at Bay site in March 2007). Despite this large variability, significant trends could be observed. Nighttime oxygen uptake increased with temperature and flow velocity. During daytime, oxygen release increased with light and also with flow velocity (Fig. 5). Temperature increases enhance respiration as well as production (Grant 1986; Wolfstein and Stal 2002), but these effects could not be separated in our analyses.

3.2 Cumulative Co-Spectra

The cumulative co-spectra calculated for each deployment revealed that the range of frequencies contributing to the flux varied between sites and over short and long time scales. For the Bay June 27, 2011, deployment (Day 1, Fig. 6), the co-spectra indicate that waves were prevalent throughout the entire deployment, and their influence on the oxygen flux is reflected in the steep and consistent slope of the spectra over a range of 0.4–1 Hz. In the presence of waves, a small misalignment between sensors can cause error in flux calculations (Berg et al. 2015), but the lack of a large dip in the co-spectra below zero at higher frequencies indicates that time lag was not a concern (Berg et al. 2013). On the

Table 3 Oxygen fluxes measured at the Bay and Gulf sites. Error estimates represent the standard error

Date	Bay		Gulf	
	Oxygen release (mmol m^{-2} day^{-1})	Oxygen uptake (mmol m^{-2} day^{-1})	Oxygen release (mmol m^{-2} day^{-1})	Oxygen uptake (mmol m^{-2} day^{-1})
Apr 08	294 ± 29	−298 ± 24		
Apr 09	204 ± 29	−217 ± 27	225 ± 72	−448 ± 50
May 10	122 ± 15	−45 ± 4		
Average spring	207 ± 50	−187 ± 75	225	−448
June 09			45 ± 11	−328 ± 28
June 10			139 ± 17	
June 11		−39 ± 10		−331 ± 12
June 11	18 ± 5	−17 ± 5	33 ± 6	−29 ± 8
July 10				−46 ± 3
Average summer	18	−28 ± 11	72 ± 34	−184 ± 84
Sept 11			363 ± 60	
Oct 10				−91 ± 7
Average fall	N/A	N/A	363	−91
Dec 11			150 ± 17	−55 ± 10
Feb 11		−35 ± 4		
Mar 07	206 ± 12		100 ± 26	
Mar 07	75 ± 8		136 ± 18	
Mar 07	189 ± 10			
Mar 09	190 ± 31	−448 ± 26	35 ± 4	−27 ± 10
Average winter	165 ± 30	−242 ± 207	105 ± 26	−41 ± 14
Annual average	130 ± 57	−152 ± 64	191 ± 66	−191 ± 45

following day (Day 2), when the significant wave height and velocity were both lower, the relatively shallow slope of the average co-spectrum, and hence, broader range of frequencies (0.014–1 Hz), indicate a combination of turbulence- and wave-driven fluxes.

4 Discussion

Average annual oxygen release and uptake (mean ± standard error) were 130 ± 57 and −152 ± 64 mmol m^{-2} day^{-1} at the Bay sites and 191 ± 66 and −191 ± 45 mmol m^{-2} day^{-1} at the Gulf sites, respectively, which can be considered moderate to high fluxes when compared to other coastal environments with permeable sediment (Tables 3, 4). The ratio of average oxygen release to uptake at both sites was close to 1 (Bay: 0.9, Gulf: 1.0), suggesting that the benthic systems were closely balanced. High rates of benthic oxygen release were recorded in spring and fall, which suggests that spring and fall microphytobenthos blooms may

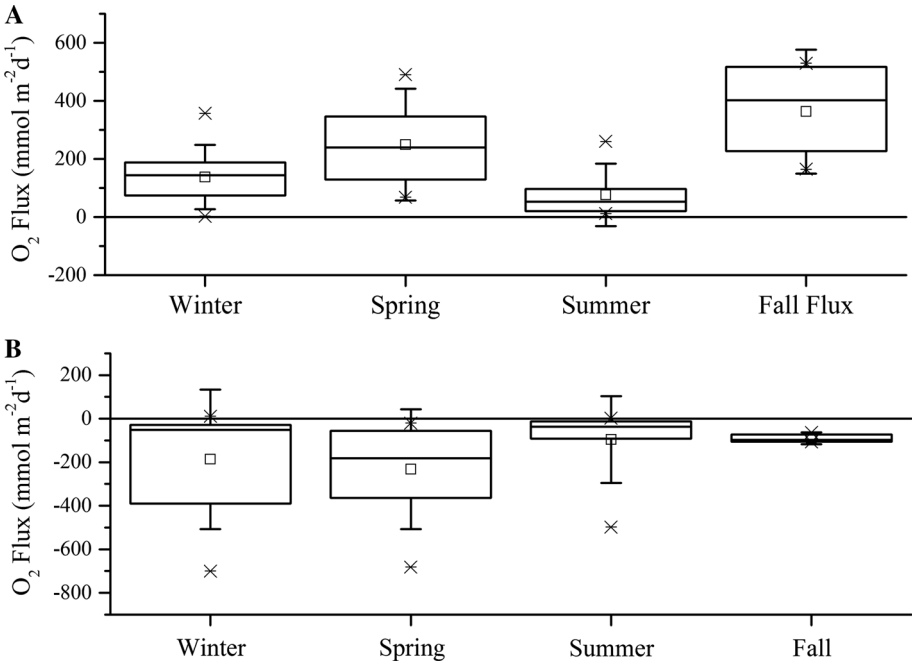

Fig. 4 *Box plots* for 14.5-min averaged seasonal fluxes combined from all study sites. Because the magnitudes of the fluxes at the Gulf and Bay sites were not significantly different, all data were combined in this graph to show general trends. **A** Oxygen release; **B** oxygen up take. The *boxplot* divides the data set into quartiles, and the *boxes* outline the data from the first (25 %) to the third (75 %) quartile. The *small squares* inside the *boxes* indicate means; *horizontal lines* inside *boxes* the medians. The ends of the *whiskers* represent one standard deviation above and below the mean. *Crossed X*s indicate data points that fell beyond the *upper* or *lower whiskers*

have supported these fluxes as seen in other coastal systems (Asmus and Bauerfeind 1994; Blanchard et al. 1997; Macintyre et al. 1996). Freshwater input from the Apalachicola River reaches maximum rates in March (Fig. 1B), and this river discharge is a major nutrient source for this region, as reflected by the Apalachicola Bay nutrient concentrations, which exceed those of the adjacent Gulf by one order of magnitude (Hallas and Huettel 2013; Mortazavi et al. 2000a, b). Decreasing nutrient input after spring results in a decline in benthic primary production rates, and we measured the lowest sedimentary oxygen release in summer with a minimum daily value of 18 ± 5 mmol m^{-2} day^{-1} in the Bay and 33 ± 6 mmol m^{-2} day^{-1} in the Gulf. These minima coincided with low oxygen uptake rates of -17 ± 5 mmol m^{-2} day^{-1} at the Bay and -29 ± 8 mmol m^{-2} day^{-1} at the Gulf sites, suggesting a tight coupling of production and respiration. As carbon availability is the ultimate driver of microbial respiration, the amount of labile carbon produced during the day via benthic photosynthesis can strongly affect nighttime sediment respiration rates.

The oxygen release and uptake rates measured during summer still are relatively high for subtropical coastal systems and similar to rates reported from temperate and boreal coastal environments (Hargrave et al. 1983; Krause-Jensen et al. 2012; Meyercordt et al. 1999), which we attribute to the vicinity of the study sites to the Apalachicola river outflow that supplies the region with nutrients. In addition, the eddy covariance method includes

Table 4 Oxygen production and uptake in sandy shelf environments

Site/environment	Sediment type	Method	O_2 production (mmol m^{-2} day^{-1})	O_2 uptake (mmol m^{-2} day^{-1})	References
German Bight	Organic C-poor sandy shelf sediments	Benthic chambers		−31.3 ± 18.2	Janssen et al. (2005)
South Atlantic Bight off Wassaw Sound, GA and St. Augustine, FL	Non-accumulating highly permeable sands	Benthic chambers	33.3 ± 21.7	−34.7 ± 23.8	Jahnke et al. (2000)
South Atlantic Bight 27 m station	Non-accumulating highly permeable sands	Core incubations	44.1	−56.9	Jahnke et al. (2005)
Middle Atlantic Bight	Organic-poor, permeable shelf sands	Percolated core incubations		−120 (May) −75 (July)	Rusch et al. (2006)
Sylt-Rømø Basin, Wadden Sea/sandy intertidal	Coarse, organic-poor, highly permeable	In-situ microsensor, incubations		−105 to −175	de Beer et al. (2005)
River Wümme, Germany/river	Sandy river sediment	Eddy covariance		−210 ± 16	Berg et al. (2003)
Banzu sandflat east coast of Tokyo Bay, Japan	Well-sorted fine sand	Eddy covariance	73.3–6.6	−14.5 to 6.6	Kuwae et al. (2006)
Lake Wohlen on the Aare River (Bern, Switzerland)	River sediment	Eddy covariance		−40 ± 11	McGinnis et al. (2008)
West Falmouth Harbor/protected estuary	Well-sorted sand/sand and gravel	Eddy covariance	31–78	−15 to −29	Berg et al. (2013)
Wakulla River/spring-fed river	Sand and gravel	Eddy covariance	137 ± 18	−360 ± 24	Berg et al. (2013)
Wakulla River/spring-fed river	Sand and gravel	Benthic chambers	200 ± 39	−89 ± 13	Berg et al. (2013)
Onslow Bay, N-Carolina continental shelf	Sand	Benthic chambers	21		Cahoon and Cooke (1992)
Northeastern Gulf of Mexico	Sand	Eddy covariance		−283	Berg and Huettel (2008)
Baltic Sea	Sand	Benthic chambers	23	−46	Cook et al. (2007)
Heron Island	Carbonate sand	Benthic chambers	130	−241	Santos et al. (2011)
Debidue Flat, North Inlet estuary, S-Carolina sand flat	Coarse-grained sand	Core incubations		−27 to −170	D'Andrea et al. (2002)

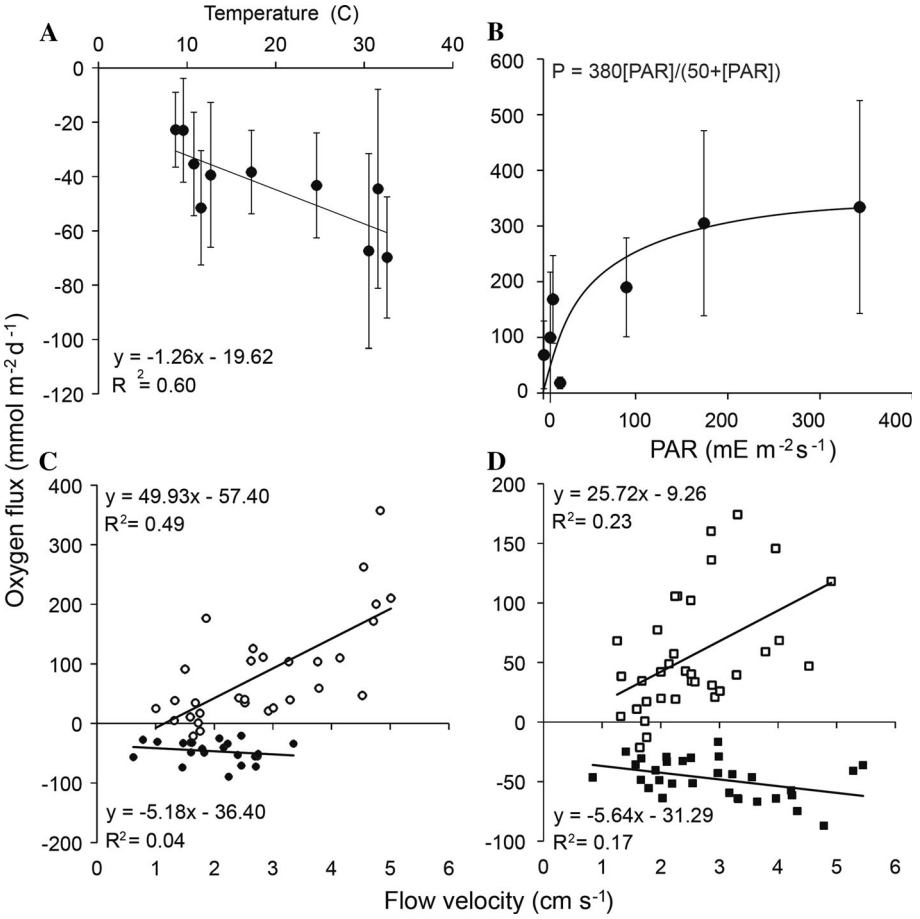

Fig. 5 **A** Effect of temperature on nighttime oxygen flux at the Bay sites ($p = 0.033$, $\alpha = 0.05$). **B** Influence of light on oxygen fluxes at the Bay sites ($p = 0.030$, $\alpha = 0.05$). **C** Effect of flow on oxygen flux at the Bay sites [*white symbols* release ($p = 0.005$, $\alpha = 0.05$); *black symbols* uptake ($p = 0.377$, $\alpha = 0.05$)] and **D** Gulf sites [release ($p = 0.002$, $\alpha = 0.05$); *black symbols* uptake ($p = 0.004$, $\alpha = 0.05$)]. *Error bars* depict one standard deviation; p values indicate significance of slope

the full effects of environmental drivers (current flow, wave action, light, etc.), and the noninvasive flux measurements thus can result in larger fluxes compared to other benthic flux measuring techniques (Berg et al. 2013).

Gulf oxygen release of 363 ± 60 mmol m^{-2} day^{-1} in September (Table 3; Bay values not available) revealed that primary production increases in fall, when increasing river discharge enhances nutrient availability and photosynthesis (Mortazavi et al. 2000a, b). Despite relatively large river discharge during winter, the decreasing light intensity and lower temperatures were likely causes for the lower production and uptake rates in the Gulf observed during winter.

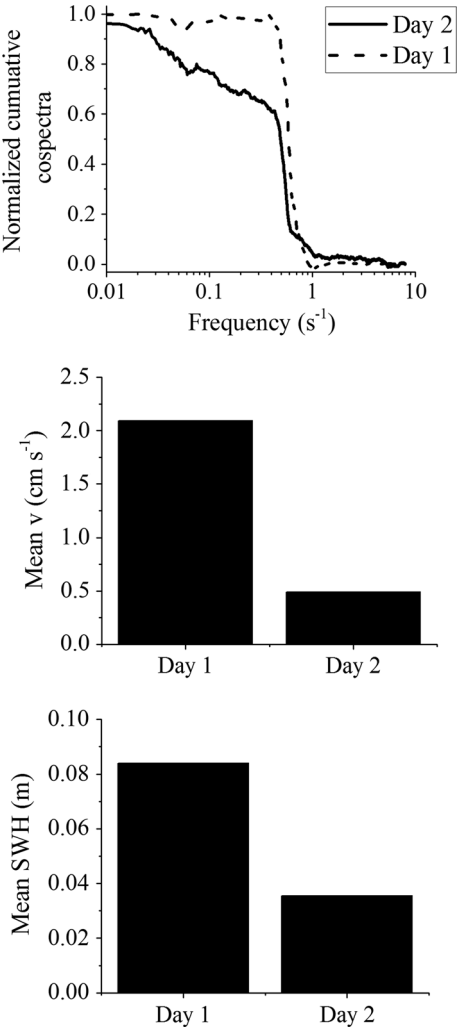

Fig. 6 Example of cumulative co-spectra measured at St. George Island Bay site on June 27 (Day 1) and 28 (Day 2) 2011. On Day 1, waves were prevalent throughout the entire deployment, reflected in the steep and consistent slope of the spectrum over the range of 0.4–1 Hz. On the following Day 2, the broader range of frequencies (0.014–1 Hz) carrying the fluxes indicate a combination of turbulence- and wave-driven fluxes

4.1 Temporal Variation

Fluxes differed between deployments conducted on consecutive days. For example, three deployments were conducted at the same location at the St. George Bay site on March 26, 27, and 30 in 2007. The mean oxygen production measured during these deployments was 206 ± 12, 75 ± 8, and 189 ± 10 mmol m^{-2} day^{-1} (mean ± standard error; $n = 4$, 10, 14), exemplifying that oxygen flux can have high daily variation, which in some instances can be as great or greater than seasonal variation.

Such variation can be caused by changes in light, temperature, and flow conditions. In shallow coastal environments, light penetrating to the bottom affects oxygen flux through its influence on biogeochemical reaction rates and photosynthesis. Despite the relatively high oxygen uptake rates of our coastal sediments, photosynthesis by microalgae led to net oxygen production during our daytime deployments, making the sediment a source of

oxygen. The reversal of flux at sunrise and sunset underlines the role of light as the dominant driver of the daily benthic oxygen flux dynamics in this shallow coastal environment (Fig. 3), in contrast to the dynamics in the deeper shelf and ocean, where the seabed is a permanent sink of oxygen.

4.2 Environmental Drivers

A consequence of the control of light on benthic oxygen dynamics is that short-term changes in light intensity can directly translate into an almost immediate change in the benthic oxygen flux. This tight coupling of light and flux has been supported by other eddy covariance studies (e.g. Berg and Huettel 2008; Berg et al. 2013; Glud et al. 2010), which demonstrate the direct effect of light variation on net ecosystem metabolism in temperate benthic environments. Further evidence of the close link between light and benthic oxygen flux dynamics can be seen in eddy covariance measurements conducted in freshwater environments (McGinnis et al. 2008), coral reefs (Long et al. 2013), seagrass meadows (Rheuban et al. 2014a, b), coralline algal beds (Attard et al. 2015), and an arctic fjord (Attard et al. 2014). However, according to the general shape of photosynthesis–irradiance curves, once a photosynthetic community becomes light saturated, changes in light availability do not substantially influence photosynthetic levels (Jasby and Platt 1976). In such instances, factors other than light (e.g., flow) can dominate the variability in oxygen release (Fig. 7).

We observed significantly higher nighttime oxygen uptake rates at higher temperatures (Fig. 5). Temperature increase can enhance heterotrophic activity through the acceleration of chemical reactions and microbial metabolic processes, and the enhancement of diffusive transport (Aller 1982; Hancke and Glud 2004; Kristensen et al. 1991). The temperature effect can be expressed by the Q_{10} temperature coefficient, which gives the change of reaction rate for an increase in temperature by 10 °C (Westrich and Berner 1984). The average Q_{10} temperature coefficient for our Bay nighttime measurements (Fig. 5A) was

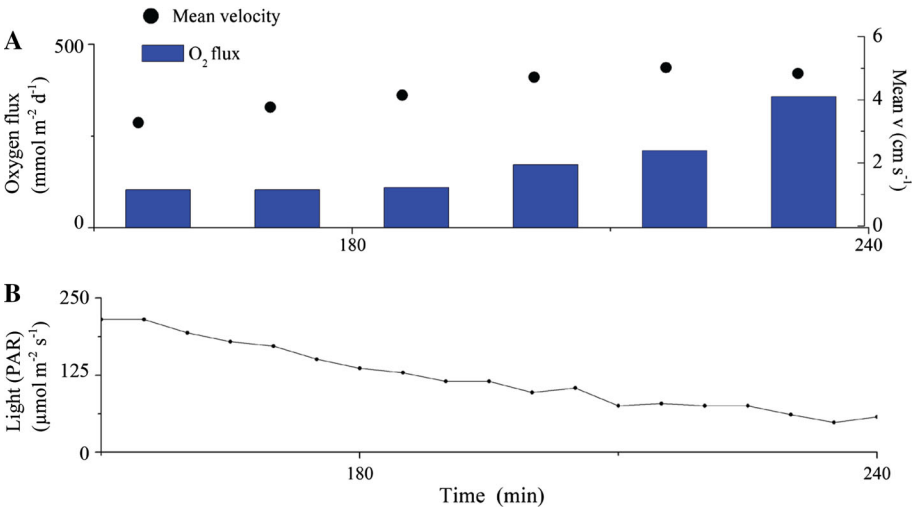

Fig. 7 **A** Oxygen release and current flow velocity (*black dots*) at the Bay site in March 2009. The response of oxygen release indicated an effect of flow velocity as opposed to an effect of light (**B**), indicating that the photosynthetic community was light saturated and did not respond to changes in light

1.4 ± 0.3 (1 SD), comparable to the Q_{10} of 1.8 reported by Thamdrup et al. (1998) for a shallow coastal sediment on the Danish coast. In sandy intertidal North Sea sediments with high benthic primary production and exposed to plankton-rich water, the Q_{10} can reach 2.7–4.3 (Kristensen et al. 1997). In sedimentary environments, the temperature effect calculated from oxygen flux is influenced by a number of variables (e.g., higher macrofauna density and activity during the warmer months of the year), and the relatively low Q_{10} value listed for our Bay site thus may have resulted from the combined effect of several processes.

Local hydrodynamics can influence the magnitude of oxygen flux, and this effect has been shown for a variety of benthic habitats (Berg et al. 2013; Long et al. 2013; Rheuban et al. 2014b; Glud et al. 2010). The effect of velocity on oxygen flux is shown in Fig. 5C, D, in which oxygen production increased with increasing flow velocity and vice versa. The scaling of oxygen flux with the magnitude of bottom current reflects the increase of solute transport into permeable sediments, which can alleviate nutrient or CO_2 limitation (for production) or organic carbon limitation (for respiration) (Precht et al. 2004; Hume et al. 2011; Cook and Røy 2006). In areas with permeable sandy sediments such as our study sites, bottom currents enhance advective pore-water flow and the associated transport of reactive substances (organic substrates and electron acceptors) into and out of the sediment (Huettel et al. 1998, 2014). For example, in June 2011, the flow velocity at Gulf Site 1 decreased from 25 to 4 cm s^{-1}, and significant wave height decreased from 8 to 3 cm over 90 min. Oxygen uptake decreased from 62 to 12 mmol m^{-2} day^{-1} (a fivefold decrease) over the same time interval (Fig. 8). Similarly, increase in oxygen release associated with increased flow can be explained by enhanced efflux of CO_2, oxygen, and/or nutrients to benthic autotrophs (Cook and Røy 2006; Carpenter and Williams 2007; Mass et al. 2010). A flow-driven effect on primary production was observed for some, but not all,

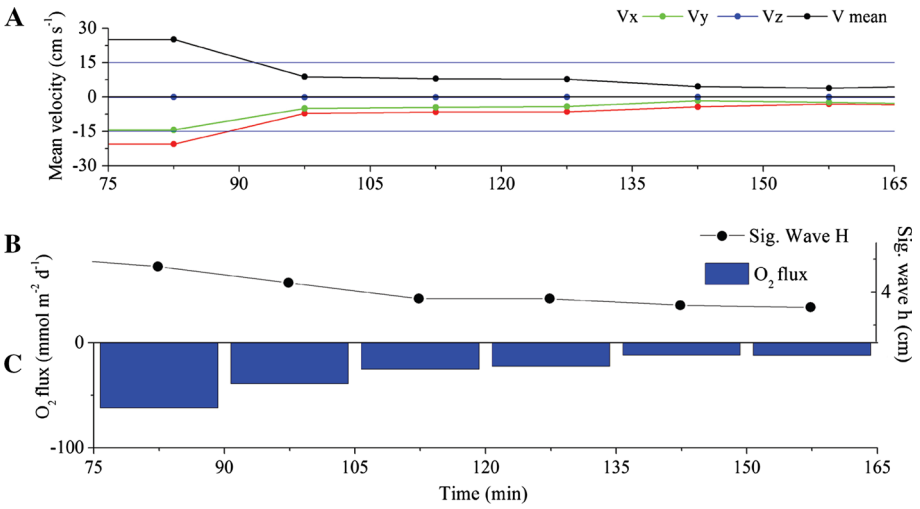

Fig. 8 **A** Decreasing bottom flow velocity and **B** significant wave height at the St. George Gulf site 1, in June 2011. **C** Corresponding decrease in sediment oxygen uptake

deployments, indicating that the CO_2, nutrient, and oxygen supply to microphytobenthos was not always a limiting factor.

4.3 Comparison with Previous Measurements

The results from our field measurements (Fig. 4) are supported by published flume experiments with controlled flow conditions. Forster et al. (1996) measured close to a doubling in total oxygen uptake in permeable sediments with an increase of flow from 3 to 14 cm s^{-1}. At the Pensacola Beach site in October 2010, a 4.5-cm increase of flow was associated with a 1.5-fold increase in oxygen uptake. At the St. George Bay Site in June 2011, a 17.5-cm decrease in flow led to a 9.5-fold decrease in oxygen uptake in the presence of only a modest decrease in velocity 0.2 cm s^{-1} over the same time interval. Likewise, eddy covariance measurements by Berg et al. (2013) in a sandy sublittoral area at the mouth of West Falmouth Harbor revealed a strong relationship between bottom currents and oxygen flux. In situ benthic advection chamber measurements set to produce defined pressure gradients at the sediment–water interface support this flow–flux relation for permeable sea beds (Janssen et al. 2005).

Where the wave base, defined as the depth at which the wave orbital water movement decreases to $\sim$4 % of the surface value (Dean and Dalrymple 1991), reaches the seafloor, wave-induced bottom flows can increase the benthic oxygen flux (Reimers et al. 2012). The shallow West Florida Shelf in the northeastern Gulf is, in general, a relatively calm region with small waves. Nevertheless, in our data series, oxygen release was significantly correlated with significant wave height for several deployments. Furthermore, in the June 2011 Bay deployment, in which larger waves were present, the eddy covariance co-spectra revealed contributions to the oxygen flux at the frequency of surface gravity waves (Day 1, Fig. 6). In an unvegetated sandy sublittoral site, Hume et al. (2011) noted a 4.5-fold increase in oxygen uptake in response to an increase in significant wave height of 19 cm. Similarly, McCann-Grosvenor et al. (2014) concluded from co-spectra of eddy covariance data collected over permeable sediments of the Oregon-Washington inner shelf that wave-induced advective transport enhances benthic oxygen flux.

Our study presents a multi-year cross-season time series of oxygen fluxes from coastal permeable sediments in the northeastern Gulf of Mexico, for which few flux data are available thus far. As the eddy covariance instrument records fluxes under undisturbed light and flow conditions, our data include the effects caused by these environmental factors and their natural temporal variability. A key characteristic of the oxygen fluxes at our sites is their tight coupling to light and current variations (Fig. 5), which we attribute primarily to the relatively high permeability of the sediment and microphytobenthic activity.

Despite the large variations, the magnitudes of our averaged fluxes are comparable to values reported for other sandy shelf environments (Table 4). Our data and the published oxygen fluxes with uptake rates of up to -10 to -283 mmol m^{-2} day^{-1} and release rates of 21–130 mmol m^{-2} day^{-1} for sandy sediments underline the role of advective pore-water exchange in supporting the high metabolic activity of these typically organic-poor sediments (<1 % dw/dw) (Boudreau et al. 2001; Huettel et al. 2014).

Our measurements produced fluxes that agree with published fluxes for similar environments; nevertheless, there are potential biases that should be considered when interpreting our data. Holtappels et al. (2013) demonstrated a potential bias in eddy covariance fluxes due changes in mean current and oxygen concentration and recommend making measurements close to the seafloor and increasing the sampling interval to 'cancel out'

biases through averaging. Our measurements were made relatively close to the seafloor (10 cm), and deployments typically covered multiple tidal cycles, and therefore, biases due to unstable environmental conditions were limited as much as possible.

Velocity effects or stirring sensitivity is an artifact inherent to Clark-type microelectrodes (Revsbech 1989; Gundersen et al. 1998; Holtappels et al. 2015; Reimers et al. 2016). Fast optodes typically do not exhibit significant correlation between turbulent flow and oxygen signal and thus are an alternative sensor for eddy covariance measurements in turbulent regimes (Holtappels et al. 2015). In our deployment at St. Joe Bay (Feb. 2011), optode sensors were used in parallel with microelectrodes, and the fluxes measured with the two systems were not significantly different (Chipman et al. 2012). These comparisons suggest that velocity effects did not cause a significant bias in our data.

Time lag between the oxygen and velocity signals can result from misalignment of the oxygen sensor from the ADV measuring volume, slow sensor response, flux-carrying eddies that are too fast to be resolved, and waves. The response time of our sensors, 0.2–0.3 s, theoretically can resolve eddies of up to 3–5 Hz. Since the frequencies of eddies measured in our systems typically were less than 1–2 Hz (Fig. 6), our sensors were able to measure the full spectrum of eddies. Furthermore, the absence of a dip in the cumulative co-spectra at higher frequencies indicates that time lag did not substantially influence the measured fluxes and a time shift correction was not needed (Berg et al. 2013, 2016).

Time lag bias in the presence of surface gravity waves is typically negligible at medium–high current velocities (>5–10 cm s^{-1}), but can cause a bias under lower flow conditions (Berg et al. 2015). Therefore, time lag bias in the presence of waves was investigated by determining whether a small time shift of 0.2 s significantly altered the flux (Berg et al. 2016). Alteration of the flux was found with the imposed time shift for some intervals during several deployments, but this bias was not consistent, indicating that the choppy, irregular waves at our nearshore sites caused error for some time intervals, but not others.

To confirm that no large bias affected the eddy covariance flux measurements, we compared the eddy flux measurements with benthic advection chamber measurements. The advection chamber generates a pressure gradient at the sediment–water interface that can be adjusted such that it mimics the natural pressure gradients that cause pore-water exchange in permeable beds (Huettel and Gust 1992; Janssen et al. 2005). Chamber fluxes measured in shallow environments nevertheless typically are lower than fluxes determined using eddy covariance because the chambers exclude some of the light, wave effects, and water column organic matter supply to the incubated sediment. Berg and co-workers (2013) reported that on a highly permeable shallow sand bed exposed to high current velocity, chambers produced up to fourfold lower oxygen fluxes than parallel eddy covariance measurements. McGinnis et al. (2014) reported O_2 fluxes measured with benthic chambers that were 1.5-fold lower than those measured with eddy covariance for permeable North Sea sediment. Advection chambers thus can produce useful conservative estimates of benthic flux and have been successfully used in numerous environments with permeable silicate or carbonate sands (Huettel et al. 2003; Huettel and Rusch 2000; Janssen et al. 2005; Wild et al. 2005, 2009).

We deployed advection chambers with an inner diameter of 19 cm and 15 cm height using an oxygen sensor (Hach optode) integrated into the chamber lid to record the oxygen concentration changes in the enclosed water. Six of these chambers were deployed at the same study sites for 24–48 h parallel to the eddy covariance instrument at least once for each season. The fluxes recorded with the chamber incubations were mostly within the low range of the eddy covariance fluxes (Table 5) and thus supported the eddy covariance measurements. Where chamber fluxes were so low that they did not overlap with the eddy fluxes (four cases), increases in bottom current during the chamber deployment likely

Table 5 Comparison of the ranges of oxygen fluxes measured with eddy covariance and advection chambers

	Oxygen release (mmol m^{-2} day^{-1})		Oxygen uptake (mmol m^{-2} day^{-1})		Oxygen release (mmol m^{-2} day^{-1})		Oxygen uptake (mmol m^{-2} day^{-1})	
	Bay eddy	Bay chambers	Bay eddy	Bay chambers	Gulf eddy	Gulf chambers	Gulf eddy	Gulf chambers
Spring	122–294	14–83	−45 to −298	−31 to −68	225	39–262	−448	−23 to −74
Summer	18	13–250	−17 to −39	−55 to −102	33–139	66–279	−46 to −328	−36 to −126
Fall	N/A	N/A	N/A	N/A	363	175	−91	N/A
Winter	75–206	58–106	−35 to −448	−22 to −181	35–150	37–63	−27 to −55	−2 to −29

caused the larger discrepancies. Because the stirring in the chambers is adjusted to the hydrodynamic conditions present at the beginning of the deployment and then remains constant throughout the incubation, a substantial increase or decrease in flow during the deployment period can lead to flux under- or overestimations when the chambers are deployed on permeable sediments, where flow can generate advective pore-water exchange (Huettel and Gust 1992). In studies where chambers were deployed on fine-grained deep sea sediments, where advective pore-water exchange is not a factor, eddy covariance and chamber measurements have shown good agreement (Berg et al. 2003, 2009; Glud et al. 2010; Donis et al. 2016). Further details of our chamber measurements will be reported elsewhere.

5 Conclusions

The average flux values reported here (overall Bay release: 130 ± 57 mmol m^{-2} day^{-1}, uptake: −152 ± 64 mmol m^{-2} day^{-1}, overall Gulf release: 191 ± 66 mmol m^{-2} day^{-1}, uptake: −191 ± 45 mmol m^{-2} day^{-1}) are within the range of fluxes previously reported for coastal environments with permeable sediment, though fluxes for specific deployments were sometimes higher. These measurements demonstrate the large ranges and variability that exist in response to natural environmental factors in coastal areas with permeable sediment, which can be higher than seasonal variability. As a result, to gain an accurate representation of oxygen flux at a single site, measurements must be integrated over representative time scales.

The annual average oxygen release to uptake ratio at both sites was close to 1 (Bay: 0.9, Gulf: 1.0), i.e., close to a state of ecological carbon equilibrium, with similar rates of production and uptake. These ratios suggest that the organic input to the sediment is highly degradable and results in high rates of oxygen respiration within the top sediment layer.

The findings emphasize the role of permeable sediments as effective biological converters for organic matter, as well as the influence of light, temperature, waves and bottom water currents on oxygen fluxes and metabolism in inner shelf sandy sediments. Our results contribute to the currently sparse knowledge on carbon turnover rates in permeable sediments, which cover the majority of the continental shelf. Because the carbon turnover rates in these areas are relatively high compared with the deep ocean, they can have a profound influence on the fate of carbon on a global scale (Huettel et al. 2014). Despite high daily, monthly, and seasonal variations in oxygen flux caused by environmental controls at our sites, the amount of oxygen released through photosynthesis is roughly balanced by uptake through respiration and oxidation process. Future research may consider what controls have the potential to alter the metabolic equilibrium of permeable sediments and how changes in these factors might be avoided. The fluxes measured in this project contribute to baseline data in a region with rapid coastal development and can help to assess whether sediment oxygen uptake and release change due to anthropogenic activities.

Acknowledgments We thank Pascal Brignole, Natalie Geyer, Chiu Cheng, Andrew Hume, John Kaba, Matt Long, Cedric Magen, Lee Russell, Mike Santema, and Brian Wells for help with the fieldwork and laboratory analyses. We also would like to thank all the volunteers that helped with instrument deployments and sample collection. This research was supported by funding from NSF Projects OCE-424967, OCE-536431, OCE-0758446, OCE-1061110 and OCE-1334117.

References

Aller RC (1982) The effects of macrobenthos on chemical properties of marine sediment and overlying water. In: McCall PL, Tevesz MJS (eds) Animal-sediment relations. Plenum Press, New York

Asmus RM, Bauerfeind E (1994) The microphytobenthos of konigshafen—spatial and seasonal distribution on a sandy tidal flat. Helgol Meeresunters 48:257–276. doi:10.1007/bf02367040

Attard KM, Glud RN, McGinnis DF, Rysgaard S (2014) Seasonal rates of benthic primary production in a Greenland fjord measured by aquatic eddy correlation. Limnol Oceanogr 59:1555–1569

Attard KM, Stahl H, Kamenos NA, Turner G, Burdett HL, Glud RN (2015) Benthic oxygen exchange in a live coralline algal bed and an adjacent sandy habitat: an eddy covariance study. Mar Ecol Prog Ser 535:99–115

Berg P, Huettel M (2008) Monitoring the seafloor using the noninvasive eddy correlation technique: integrated benthic exchange dynamics. Oceanography 21:164–167

Berg P, Roy H, Janssen F, Meyer V, Jorgensen BB, Huettel M, de Beer D (2003) Oxygen uptake by aquatic sediments measured with a novel non-invasive eddy-correlation technique. Mar Ecol Prog Ser 261:75–83

Berg P, Glud RN, Hume A, Stahl H, Oguri K, Meyer V, Kitazato H (2009) Eddy correlation measurements of oxygen uptake in deep ocean sediments. Limnol Oceanogr Methods 7:576–584. doi:10.4319/lom.2009.7.576

Berg P et al (2013) Eddy correlation measurements of oxygen fluxes in permeable sediments exposed to varying current flow and light. Limnol Oceanogr 58:1329–1343. doi:10.4319/lo.2013.58.4.1329

Berg P, Reimers CE, Rosman JE, Huettel M, Delgard ML, Reidenbach MA, Özkan-Haller HT (2015) Technical note: time lag correction of aquatic eddy covariance data measured in presence of waves. Biogeosciences 12:6721–6735. doi:10.5194/bg-12-6721-2015

Berg P, Koopmans DJ, Huettel M, Li H, Mori K, Wüest A (2016) A new robust oxygen–temperature sensor for aquatic eddy covariance measurements. Limnol Oceanogr Methods 14:151–167. doi:10.1002/lom3.10071

Blanchard GF, Guarini JM, Gros P, Richard P (1997) Seasonal effect on the relationship between the photosynthetic capacity of intertidal microphytobenthos and temperature. J Phycol 33:723–728. doi:10.1111/j.0022-3646.1997.00723.x

Boudreau BP et al (2001) Permeable marine sediments: overturning an old paradigm. EOS Trans Am Geophys Union 82:133–136

Businger JA (1986) Evaluation of the accuracy with which dry deposition can be measured with current micrometeorological techniques. J Clim Appl Meteorol 25:1100–1124

Cahoon LB (1999) The role of benthic microalgae in neritic ecosystems. Oceanogr Mar Biol 37:47–86

Cahoon LB, Cooke JE (1992) Benthic microalgal production in Onslow Bay, North Carolina, USA. Mar Ecol Prog Ser 84:185–196

Canfield DE, Jørgensen BB, Fossing H, Glud R, Gundersen J et al (1993) Pathways of organic carbon oxidation in three continental margin sediments. Mar Geol 113:27–40

Carpenter R, Williams S (2007) Mass transfer limitation of photosynthesis of coral reef algal turfs. Mar Biol 151:435–450

Chipman L, Podgorski D, Green S, Kostka J, Cooper W, Huettel M (2010) Decomposition of plankton-derived dissolved organic matter in permeable coastal sediments. Limnol Oceanogr 55:857–871

Chipman L, Huettel M, Berg P, Meyer V, Klimant I, Glud RN, Wenzhoefer F (2012) Oxygen optodes as fast sensors for eddy correlation measurements in aquatic systems. Limnol Oceanogr Methods 10:304–316

Cook PLM, Røy H (2006) Advective relief of CO_2 limitation in highly productive sandy sediments. Limnol Oceanogr 51:1594–1601

Cook PLM, Wenzhöfer F, Glud RN, Janssen F, Huettel M (2007) Benthic solute exchange and carbon mineralization in two shallow subtidal sandy sediments: effect of advective pore-water exchange. Limnol Oceanogr 52:1943–1963

D'Andrea AF, Aller RC, Lopez GR (2002) Organic matter flux and reactivity on a South Carolina sandflat: the impacts of porewater advection and macrobiological structures. Limnol Oceanogr 47:1056–1070

de Beer D, Wenzhöefer F, Ferdelman TG, Boehme SE, Huettel M et al (2005) Transport and mineralization rates in North Sea intertidal sediments, Sylt-Rømø Basin, Wadden Sea. Limnol Oceanogr 50(1):113–127

Dean RG, Dalrymple RA (1991) Water wave mechanics for engineers and scientists. Advanced series on ocean engineering 2. World Scientific, Singapore

Donis D et al (2015) An assessment of the precision and confidence of aquatic eddy correlation measurements. J Atmos Ocean Technol 32:642–655. doi:10.1175/JTECH-D-14-00089.1

Donis D, McGinnis DF, Holtappels M, Felden J, Wenzhöefer F (2016) Assessing benthic oxygen fluxes in oligotrophic deep sea sediments (HAUSGARTEN observatory). Deep-Sea Res Part I Oceanogr Res Pap 111:1–10

Forster S, Huettel M, Ziebis W (1996) Impact of boundary layer flow velocity on oxygen utilisation in coastal sediments. Mar Ecol Prog Ser 146:173–185

Forster S, Glud RN, Gundersen JK, Huettel M (1999) In situ study of bromide tracer and oxygen flux in coastal sediments. Estuar Coast Shelf Sci 49:813–827

Gattuso JP, Gentili B, Duarte CM, Kleypas JA, Middelburg JJ, Antoine D (2006) Light availability in the coastal ocean: impact on the distribution of benthic photosynthetic organisms and their contribution to primary production. Biogeosciences 3:489–513

Glud RN (2008) Oxygen dynamics of marine sediments. Mar Biol Res 4:243–289

Glud RN, Berg P, Hume A, Batty P, Blicher ME, Lennert K, Rysgaard S (2010) Benthic O2 exchange rates across hard-bottom substrates quantified by eddy correlation in a sub-Arctic fjord system. Mar Ecol Prog Ser 417:1–12

Grant J (1986) Sensitivity of benthic community respiration and primary production to changes in temperature and light. Mar Biol 90:299–306

Grasshoff K, Kremling K, Ehrhardt M (1999) Methods of seawater analysis, 3rd edn. Wiley-VCH, Weinheim

Gundersen JK, Ramsing NB, Glud RN (1998) Predicting the signal of O-2 microsensors from physical dimensions, temperature, salinity, and O-2 concentration. Limnol Oceanogr 43:1932–1937

Hallas MK, Huettel M (2013) Bar-built estuary as a buffer for riverine silicate discharge to the coastal ocean. Cont Shelf Res 55:76–85. doi:10.1016/j.csr.2013.01.011

Hancke K, Glud RN (2004) Temperature effects on respiration and photosynthesis in three diatom-dominated benthic communities. Aquat Microb Ecol 37:265–281

Hargrave BT, Prouse NJ, Phillips GA, Neame PA (1983) primary production and respiration in pelagic and benthic communities at 2 intertidal sites in the upper bay of fundy. Can J Fish Aquat Sci 40:229–243

He RY, Weisberg AH (2002) Tides on the West Florida shelf. J Phys Oceanogr 32:3455–3473

Holtappels M, Glud RN, Donis D, Liu B, Hume A, Wenzhöfer F, Kuypers M (2013) Effects of transient bottom water currents and oxygen concentrations on benthic exchange rates as assessed by eddy correlation measurements. J Geophys Res Oceans 118:1157–1169. doi:10.1002/jgrc.20112

Holtappels M, Noss Hancke K, Cathalot C, McGinnis DF, Lorke A, Glud RN (2015) Aquatic eddy correlation: quantifying the artificial flux caused by stirring-sensitive O_2 sensors. PLoS ONE 10:e0116564. doi:10.1371/journal.pone.0116564

Huang WR, Spaulding M (2002) Modelling residence-time response to freshwater input in Apalachicola Bay, Florida, USA. Hydrol Process 16:3051–3064

Huettel M, Gust G (1992) Impact of bioroughness on interfacial solute exchange in permeable sediments. Mar Ecol Prog Ser 89:253–267

Huettel M, Rusch A (2000) Transport and degradation of phytoplankton in permeable sediment. Limnol Oceanogr 45:534–549

Huettel M, Webster IT (2000) Porewater flow in permeable sediment. In: Boudreau BP, Jørgensen BB (eds) The benthic boundary layer: transport processes and biogeochemistry. Oxford University Press, Oxford, pp 144–179

Huettel M, Ziebis W, Forster S, Luther GW (1998) Advective transport affecting metal and nutrient distributions and interfacial fluxes in permeable sediments. Geochim Cosmochim Acta 62:613–631

Huettel M, Røy H, Precht E, Ehrenhauss S (2003) Hydrodynamical impact on biogeochemical processes in aquatic sediments. Hydrobiologia 494:231–236

Huettel M, Berg P, Kostka JE (2014) Benthic exchange and biogeochemical cycling in permeable sediments. Annu Rev Mar Sci 6(6):23–51. doi:10.1146/annurev-marine-051413-012706

Hume AC, Berg P, McGlathery KJ (2011) Dissolved oxygen fluxes and ecosystem metabolism in an eelgrass (*Zostera marina*) meadow measured with the eddy correlation technique. Limnol Oceanogr 56:86–96. doi:10.4319/lo.2011.56.1.0086

Jahnke RA, Marinelli RL, Eckmann JE, Nelson JR (1996) Pore water nutrient distributions in non-accumulating, sandy sediments of the South Atlantic Bight continental shelf. EOS 76:202

Jahnke RA, Nelson JR, Marinelli RL, Eckman JE (2000) Benthic flux of biogenic elements on the Southeastern US continental shelf: influence of pore water advective transport and benthic microalgae. Cont Shelf Res 20:109–127

Jahnke R, Richards M, Nelson J, Robertson C, Rao A, Jahnke D (2005) Organic matter remineralization and porewater exchange rates in permeable South Atlantic Bight continental shelf sediments. Cont Shelf Res 25:1433–1452. doi:10.1016/j.csr.2005.04.002

Jahnke RA, Nelson JR, Richards ME, Robertson CY, Rao AMF, Jahnke DB (2008) Benthic primary productivity on the Georgia midcontinental shelf: benthic flux measurements and high-resolution, continuous in situ PAR records. J Geophys Res 113:C08022. doi:10.1029/2008JC004745

Janssen F, Huettel M, Witte U (2005) Pore-water advection and solute fluxes in permeable marine sediments (II): benthic respiration at three sandy sites with different permeabilities (German Bight, North Sea). Limnol Oceanogr 50:779–792

Jasby AD, Platt T (1976) Mathematical formulation of the relationship between photosynthesis and light for phytoplankton. Limnol Oceanogr 21:540–547

Krause-Jensen D, Markager S, Dalsgaard T (2012) Benthic and pelagic primary production in different nutrient regimes. Estuar Coasts 35:527–545. doi:10.1007/s12237-011-9443-1

Kristensen E, Aller RC, Aller JY (1991) Oxic and anoxic decomposition of tubes from the burrowing sea anemone *Ceriantheopsis americanus*—implications for bulk sediment carbon and nitrogen balance. J Mar Res 49:589–617

Kristensen E, Jensen MH, Jensen KM (1997) Temporal variations in microbenthic metabolism and inorganic nitrogen fluxes in sandy and muddy sediments of a tidally dominated bay in the northern Wadden Sea. Helgol Meeresunters 51:295–320. doi:10.1007/bf02908717

Kuwae T, Kamio K, Inoue T, Miyoshi E, Uchiyama Y (2006) Oxygen exchange flux between sediment and water in an intertidal sandflat, measured in situ by the eddy-correlation method. Mar Ecol Prog Ser 307:59–68

Lee X, Massman W, Law B (2004) Handbook of micro-meteorology: a guide for surface flux measurement and analysis. Kluwer Academic Publishers, Dordrecht

Long MH, Berg P, de Beer D, Zieman JC (2013) In situ coral reef oxygen metabolism: an eddy correlation study. PLoS ONE. doi:10.1371/journal.pone.0058581

Long MH, Berg P, McGlathery K, Zieman JC (2015) Sub-tropical seagrass ecosystem metabolism measured by eddy covariance. Mar Ecol Prog Ser 529:75–90. doi:10.3354/meps11314

Lorke A, McGinnis DF, Maeck A (2013) Eddy-correlation measurements of benthic fluxes under complex flow conditions: effects of coordinate transformations and averaging time scales. Limnol Oceanogr Methods 11:425–437. doi:10.4319/lom.2013.11.425

Lorrai C, McGinnis DF, Brand A, Wüest A (2010) Application of oxygen eddy correlation in aquatic systems. J Atmos Ocean Technol 27:1533–1546. doi:10.1175/2010JTECHO723.1

Macintyre HL, Geider RJ, Miller DC (1996) Microphytobenthos: the ecological role of the "secret garden" of unvegetated, shallow-water marine habitats. 1. Distribution, abundance and primary production. Estuaries 19:186–201

Mass T, Genin A, Shavit U, Grinstein M, Tchernov D (2010) Flow enhances photosynthesis in marine benthic autotrophs by increasing the efflux of oxygen from the organism to the water. PNAS 107(6):2527–2531

McCann-Grosvenor K, Reimers CE, Sanders RD (2014) Dynamics of the benthic boundary layer and seafloor contributions to oxygen depletion on the Oregon inner shelf. Cont Shelf Res 84:93–106. doi:10.1016/j.csr.2014.05.010

McGinnis DF, Berg P, Brand A, Lorrai C, Edmonds TJ, Wuest A (2008) Measurements of eddy correlation oxygen fluxes in shallow freshwaters: towards routine applications and analysis. Geophys Res Lett. doi:10.1029/2007gl032747

McGinnis DF, Sommer S, Lorke A, Glud RN, Linke P (2014) Quantifying tidally driven benthic oxygen exchange across permeable sediments: an aquatic eddy correlation study. J Geophys Res 119:6918–6932

Mermillod-Blondin F, Francois-Carcaillet F, Rosenberg R (2005) Biodiversity of benthic invertebrates and organic matter processing in shallow marine sediments: an experimental study. J Exp Mar Biol Ecol 315:187–209

Meyercordt J, Gerbersdorf S, Meyer-Reil LA (1999) Significance of pelagic and benthic primary production in two shallow coastal lagoons of different degrees of eutrophication in the southern Baltic Sea. Aquat Microb Ecol 20:273–284. doi:10.3354/ame020273

Morey SL, Dukhovskoy DS, Bourassa MA (2009) Connectivity of the Apalachicola River flow variability and the physical and bio-optical oceanic properties of the northern West Florida Shelf. Cont Shelf Res 29:1264–1275. doi:10.1016/j.csr.2009.02.003

Mortazavi B, Iverson RL, Huang WR, Lewis FG, Caffrey JM (2000a) Nitrogen budget of Apalachicola Bay, a bar-built estuary in the northeastern Gulf of Mexico. Mar Ecol Prog Ser 195:1–14

Mortazavi B, Iverson RL, Landing WM, Huang WR (2000b) Phosphorus budget of Apalachicola Bay: a river-dominated estuary in the northeastern Gulf of Mexico. Mar Ecol Prog Ser 198:33–42

Precht E, Franke U, Polerecky L, Huettel M (2004) Oxygen dynamics in permeable sediments with wave-driven pore water exchange. Limnol Oceanogr 49:693–705. doi:10.4319/lo.2004.49.3.0693

Reimers CE, Özkan-Haller T, Berg P, Devol A, McCann-Grosvenor K, Sanders RD (2012) Benthic oxygen consumption rates during hypoxic conditions on the Oregon continental shelf: evaluation of the eddy correlation method. J Geophys Res 117:1–18. doi:10.1029/2011JC007564

Reimers CE, Ozkan-Haller T, Albright A, Berg P (2016) Microelectrode velocity effects and aquatic eddy covariance measurements under waves. J Atmos Ocean Technol 33:263–282

Revsbech NP (1989) An oxygen microsensor with a guard cathode. Limnol Oceanogr 34:474–478

Rheuban JE, Berg P, McGlathery KJ (2014a) Ecosystem metabolism along a colonization gradient of eelgrass (*Zostera marina*) measured by eddy correlation. Limnol Oceanogr 59:1376–1387. doi:10.4319/lo.2014.59.4.1376

Rheuban JE, Berg P, McGlathery KJ (2014b) Multiple timescale processes drive ecosystem metabolism in eelgrass (*Zostera marina*) meadows. Mar Ecol Prog Ser 507:1–13. doi:10.3354/meps10843

Riedl R, Huang N, Machan R (1972) The subtidal pump: a mechanism of interstitial water exchange by wave action. Mar Biol 13:210–221

Rusch A, Huettel M, Wild C, Reimers CE (2006) Benthic oxygen consumption and organic matter turnover in organic-poor, permeable shelf sands. Aquat Geochem 12:1–19

Santema M, Clarke AJ, Speer K, Huettel M (2015) Water column oxygen dynamics within the coastal gradient in the northeastern Gulf of Mexico inner shelf. Cont Shelf Res 104:104–119. doi:10.1016/j.csr.2015.05.006

Santos IR, Glud RN, Maher D, Erler D, Eyre BD (2011) Diel coral reef acidification driven by porewater advection in permeable carbonate sands, Heron Island, Great Barrier Reef. Geophys Res Lett 38:L03604

Snyder RA et al (2014a) Polycyclic aromatic hydrocarbon concentrations across the Florida Panhandle continental shelf and slope after the BP MC 252 well failure. Mar Pollut Bull 89:201–208. doi:10.1016/j.marpolbul.2014.09.057

Snyder RA, Vestal A, Welch C, Barnes G, Pelot R, Ederington-Hagy M, Hileman F (2014b) PAH concentrations in Coquina (*Donax* spp.) on a sandy beach shoreline impacted by a marine oil spill. Mar Pollut Bull 83:87–91. doi:10.1016/j.marpolbul.2014.04.016

Thamdrup B, Hansen JW, Jorgensen BB (1998) Temperature dependence of aerobic respiration in a coastal sediment. FEMS Microbiol Ecol 25:189–200. doi:10.1016/s0168-6496(97)00095-0

Wenzhofer F, Glud RN (2004) Small-scale spatial and temporal variability in coastal benthic O-2 dynamics: effects of fauna activity. Limnol Oceanogr 49:1471–1481

Westrich JT, Berner RA (1984) The role of sedimentary organic matter in bacterial sulfate reduction: the G model tested. Limnol Oceanogr 29:236–249

Wild C, Rasheed M, Jantzen C, Cook P, Struck U, Huettel M, Boetius A (2005) Benthic metabolism and degradation of natural particulate organic matter in carbonate and silicate reef sands of the northern Red Sea. Mar Ecol Prog Ser 298:69–78

Wild C, Naumann MS, Haas A, Struck U, Mayer FW, Rasheed MY, Huettel M (2009) Coral sand O-2 uptake and pelagic-benthic coupling in a subtropical fringing reef, Aqaba, Red Sea. Aquatic Biology 6:133–142

Wolfstein K, Stal LJ (2002) Production of extracellular polymeric substances (EPS) by benthic diatoms: effect of irradiance and temperature. Mar Ecol Prog Ser 236:13–22

Zavala-Hidalgo J, Romero-Centeno R, Mateos-Jasso A, Morey SL, Martinez-Lopez B (2014) The response of the Gulf of Mexico to wind and heat flux forcing: what has been learned in recent years? Atmosfera 27:317–334

Ziebis W, Forster S, Huettel M, Jorgensen BB (1996a) Complex burrows of the mud shrimp *Callianassa truncata* and their geochemical impact in the sea bed (vol 382, pg 619, 1996). Nature 383:457

Ziebis W, Huettel M, Forster S (1996b) Impact of biogenic sediment topography on oxygen fluxes in permeable seabeds. Mar Ecol Prog Ser 140:227–237